A General Approach for the Reconstruction of Complex Buildings from 3D Pointclouds Using Bayesian Networks and Cellular Automata

Maria Chizhova [a], Dmitrii Korovin [b], Andrey Gurianov [c], Ansgar Brunn [d], Thomas Luhmann [e] and Uwe Stilla [f]

[a] Technical University of Munich/University of Applied Sciences Würzburg-Schweinfurt /Jade University Oldenburg; Germany; mariatschishowa@yahoo.de
[b] Ivanovo State University of Power Engineering, Ivanovo, Russia; dmitriyikorovin@list.ru
[c] Ivanovo State University, Ivanovo, Russia; a.v.gur.2008@mail.ru
[d] University of Applied Sciences Würzburg-Schweinfurt, Würzburg, Germany; ansgar.brunn@fhws.de
[e] Jade University of Applied Sciences, Oldenburg, Germany; luhmann@jade-hs.de
[f] Technical University of Munich, Munich, Germany; uwe.stilla@tum.de

Abstract: Point cloud interpretation and reconstruction of 3D buildings from point clouds has already been addressed for a few decades. There are many articles which consider different methods and workflows of the automatic detection and reconstruction of geometrical objects from point clouds. Each method is suitable for a specific geometry type of object or sensor. General approaches are rare. In our work, we present an algorithm which develops the optimal process sequence of the automatic search, detection and reconstruction of buildings and building components from a point cloud. It can be used for the detection of sets of geometric objects to be reconstructed, regardless of the level of damage. In a real example, we reconstruct a complete Russian Orthodox church starting from a set of detected structural components and reconstruct missing components with high probability.

Keywords: reconstruction; cellular automata; Bayesian networks

---

1. Introduction

1.1. Motivation

The development of science, technology and equipment as well as the human ability to invent new constructions have allowed the creation of a large variety of different unique objects in the real world. Over time, a lot of information about former cultural objects has been lost, and some objects have been severely

damaged or ruined. Digital reconstruction makes building principles easier to understand, especially for partly destroyed or no longer existing objects. The reconstruction of lost historical and architectural objects is an up-to-date topic in many researches. Using 3D laser scanning, we can create 3D construction models of real scenes with high precision and completeness. Complex geometry reconstruction from point clouds in the context of the big data problem is not a trivial matter and needs methods and algorithms for the optimization of data processing. Due to the large amount of data, the choice of efficient methods is an important task.

As a standard rule, in the case of building reconstruction with geometrical features, object reconstruction begins with feature detection. The existing methods are mostly appropriate for simple objects such as recognition of planes or spheres. For complex objects, combining different geometric entities, the choice of one particular detection method is not always appropriate because each method offers its own advantages for specific types of geometric entities.

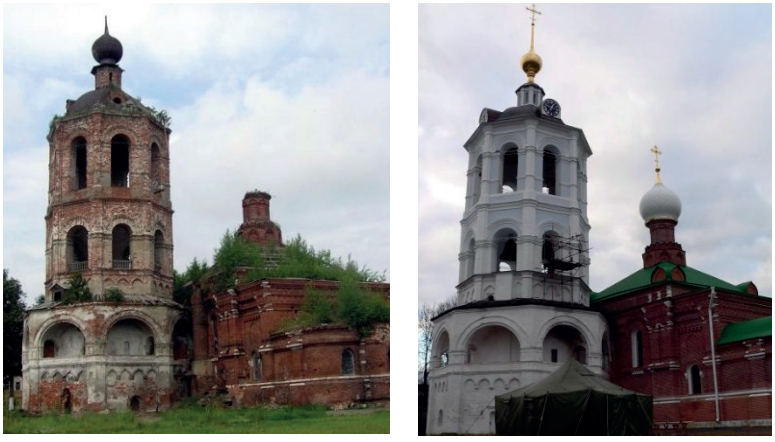

Figure 1. Reconstruction of a destroyed church.

In this article, we develop the mathematical model of a new method, which allows an optimized extraction of geometrical information from laser scanning point clouds and its efficient interpretation for further reconstruction. This method is suitable for object reconstruction from incomplete data, which can be the result of missing object parts (e.g., destroyed object) or a failed measurement process (e.g., due to reflectivity properties of an object).

This work is carried out in the context of recent research in the virtual reconstruction of destroyed orthodox churches, which are characterized by their complex architecture.

1.2. Previous Works

Considering previous work, we focus on two aspects:

1. point cloud interpretation and
2. reconstruction from precise point clouds.

In our case, point cloud interpretation means extraction of analytical, geometrical and semantical information from point clouds. Here, geometry extraction is relevant to our work. The most common techniques of geometry extraction from point clouds are as follows:

- RANSAC and its variations:
  Schnabel et al. (2007) use the RANSAC algorithm in their work for fitting geometric primitives (such as planes, spheres, etc.) from unorganized point clouds. Al-Durgham et al. (2013) search for straight lines in the point clouds for LS-point clouds registration using RANSAC. Rusu et al. (2009) use a RMSAC algorithm—Randomized M-Estimator Sample Consensus—that can be considered as an extension of RANSAC using the modified minimizing target function. The algorithm finds a best-fit geometrical surface form for the further model-based object reconstruction.
- Hough transformation (HT):
  Vosselman et al. (2004), Overby et al. (2004), Rabbani and Heuvel (2005) extract geometric primitives (planes, cylinders, spheres and cones) using 3D Hough transformation, which can be understood as an extension of the classic 2D Hough transformation. The Hough transformation is quite suitable for the detection of simple geometric forms, but it is not efficient for the detection of more complex geometries due to the increasing time involved and calculation complexity. Maltezos and Ioannidis (2016) use Randomized Hough Transformation (RHT), a probabilistic variation of classic HT based on affinity calculation between the new object (e.g., curve) and the object in the accumulator for the detection of roof planes.
- Least-squares fitting:
  The fitting of parametric curves and surfaces using least squares methods has been considered in detail by Ahn (2004) and elaborated upon by Liu and Wang (2008). Wang et al. (2004) address the problem of correct curve fitting in unorganized noisy point clouds. The algorithm is based on squared distance minimization between points of the LS point cloud and the given B-spline-curve. Fleischmann et al. (2005) present surface fitting using robust Moving Least Squares for further surface reconstruction.
- Methods of differential geometry:

a detailed description of geometrical primitives from point clouds was given in Becker (2005).

Even though these methods are quite robust, some of them are dependent on the number of processing iterations, need prior sampling and are not always correct for complex objects, which can be a combination of different geometries. In the case of complex architectures, which cannot be approximated with only single geometric primitives, the detection method of one geometric object can differ from others. The chosen method determines the further reconstruction of the whole object.

There are different reconstruction approaches based on interpreted information from point clouds. Some reconstruction methods use a strict prototype model. In many articles about reconstruction of cultural heritage objects, a library of typological architectural elements taking into account construction canons is used. In Quattrini et al. (2015), a destroyed architectural object has been completely reconstructed from the TLS point cloud as well as single classified archaeological samples according to practical and theoretical canons of roman architecture. Dore and Murphy (2013) generated digital historical models using Historic Building Information Modelling (HBIM) containing parametric library objects and procedural modelling techniques. Later on, Dore et al. (2015) developed a set of rules and algorithms for the automatic combination of parametric library objects and generation of HBIMs from survey data (historic surveys and a recent laser scan survey as segmented point cloud and cut sections). A conceptual framework is based on the definition of shape grammar, which allows for the automatic generation of 2D and 3D geometries from a basic vocabulary of shapes. The reconstruction is supported by architectural rules and proportions. There are some software applications that allow for semi-automatic modelling of architectural forms according to a library of structural elements, in which the model parameters of a structure element are estimated from user defined key points (Kivilcim and Duran, 2016).

Huang et al. (2011) developed roof decomposition rules for the reconstruction of LoD2 buildings. Based on a predefined library of primitives, generative modelling has been conducted to construct the target roof that fits the data. Extracted primitives from a point cloud were composed and merged. Nguatem et al. (2013) extracted a ridgeline from the highest points of the point cloud—bounded with a ground plan—for roof model fitting using the likelihood principle.

The reconstruction of single architectural models is considered in Canciani et al. (2013). The method is based on the extrusion path modelling of architectural elements from the point cloud section, which have been compared with a knowledge-based model.

In many articles, a building reconstruction is based on the integration of extracted geometrical information about single object parts according to different composition rules.

Extracted straight lines and planes (e.g., using RANSAC, Hough transform) often assist in planar object reconstruction and decomposition of its elements (e.g., roofs—Nizar et al. (2006), Arefi et al. (2010), buildings—Rusu et al. (2009)). Verma et al. (2006) detected planes and rectangular outlines for roof composition using a Roof Topology Graph. Kada and Wichmann (2013) generated complex building shapes using a Boolean intersection of half-spaces, which define convex building components. Xiong et al. (2015) represented roofs with topological graphs and applied the Minimum Cycles Method for roof decomposition using extracted geometrical primitives from airborne LiDAR data.

In recent years, probabilistic approaches have been widely used in recognition processes. Probabilistic graphical models (PGM), developed by Koller and Friedman (2009), integrate schematic graphical object representation (e.g., as a graph) with different stochastic statistic models, such as the Hidden Markov Model (HMM), Conditional Random Field (CRF) and Bayesian nets, allowing for probabilistic decision-making. Ruiz-Sarmiento et al. (2015) integrated PGMs as Conditional Random Fields (CRF) with Semantical Knowledge (SK) for the representation of object relations in the context of an input scene. Xiong and Huber (2010) extracted and classified planar regions for further object recognition using CRF. Anand et al. (2013) used an isomorphic to MRF (Markov Random Fields) model for object recognition and classification in certain scenes (e.g., office, house). Förstner (2013) showed the efficiency of object parameter estimation and classification, which are optimized through the implementation of Bayesian nets and MRF in the context of the flexible construction of graphical models.

In all cases, a big data problem is relevant for point cloud processing. The role of high mechanism complexity and the creation of self-reproducing intelligent automates for the acceleration of technological processes has already been discussed for many years (e.g., v. Neumann, 1966). An additional example from such automates is cellular automaton (CA)—a discrete model for the description of dynamic systems, which can be based on various rules (using, for example, Bayes theory and Bayesian networks (Wolfram (1983), Neapolitan (2004)). Since CA provides accelerated processing, this approach is favoured in our actual work.

2. The New Proposed Method

2.1. Outline of Algorithm

The developed method is based on a probabilistic approach and discrete mathematical methods, namely Bayesian networks and cellular automata theory (see Ch. 2.5). Let us consider an algorithm, which makes an automatic choice of an acceptable method for the detection of different geometrical entities in a complex object and its further automatic reconstruction from incomplete data. Thus, we consider an a priori known object configuration with its pre-defined semantic

information, which is organized like a graph. A combination of Bayesian nets with cellular automata allows one to define an optimal

- geometric candidate for object detection;
- means of recognition;
- decision-making process for reconstruction from incomplete data.

The reconstruction algorithm can be described with the following steps.

1. Pre-processing
   - creation of a database from complete churches;
   - manual church description;
   - church representation with a graph, including topological, semantic and geometrical information about some church components;
   - fusion of all church graphs into one joint graph;
   - creation of a Bayesian network based on a joint graph using frequent information about components in the database.
2. Object measurement (e.g., laser scanning)
   - object measurement (laser scanning, photogrammetric approach);
   - point cloud registration;
   - point cloud filtering;
   - cleaning.
3. Segmentation
   - segmentation of rotational objects (domes, tambour);
   - nave segmentation;
   - segmentation of simple geometries and non-rotational objects (walls, roofs etc.)
4. Topology and semantic definition of segmented church components:
   - segments connection into a topological graph;
   - semantic definition of "sure" components (nave, domes on the main roof);
   - semantic definition of "unsure" components through matching with a joint graph.
5. Geometry detection and reconstruction:
   - geometry extraction of components with "sure" semantic;
   - geometry extraction of components with "unsure" semantic and its semantic correction (using cellular automata);
   - reconstruction of destroyed or missing parts using cellular automata.

2.2. Research Object

Our research objects are stone orthodox churches. There are a considerable number of such churches in the territory of Russia, Belarus and Ukraine. Several churches have been destroyed and are not used as religious institutions any more. There is a huge interest in the restoration of these objects.

It is necessary to observe the number of canons, determined by religion during the churches' construction. These canons resulted in the evolution of the culture in that territory (and that time), in which we observe this or that church. Nevertheless, it is possible to claim that each church has a certain topological structure of some elements determined by canons. Each of these elements is geometrically characterized by its properties.

Table 1. Example of a classification library with visual models (not all models are represented).

Component	Model 1	Model 2	Model 3
crucifix (*Kr*)			
dome (*K*, *HK*)			
cylinder (*Tr*)			
roof (*D*)			
altar (*A*, *HA*, *OA*)			
nave (*X*)			

2.3. Object Classification and Representation

A database of a certain amount of churches with a classification of structural elements was built for the derivation of probabilistic relations between elements and acts as a base for further construction of a Bayesian network. In our case, the abbreviations of the church parts are (see example in Table 1): *Kr* - crucifix, *K* - dome (*HK* - main dome), *Tr* - cylinder, *St* - prop, *D* - roof, *X* - nave, OA_r - sacrifice altar right, D_r - sacrifice altar roof (right), *HA* - main altar; *D* - main altar roof, OA_l - sacrifice altar left, D_l - sacrifice altar roof (left). We model our objects—orthodox churches—with colour-oriented topological graphs $G = (V, E)$. The vertices *V* are the structural components of the church, like a cupola or a crucifix with arbitrary geometries. The edges *E* are the neighbouring relations

between the elements of V, which are attributed by conditional probabilities to the edges. The objects differ in their complexity (cf. Figure 2).

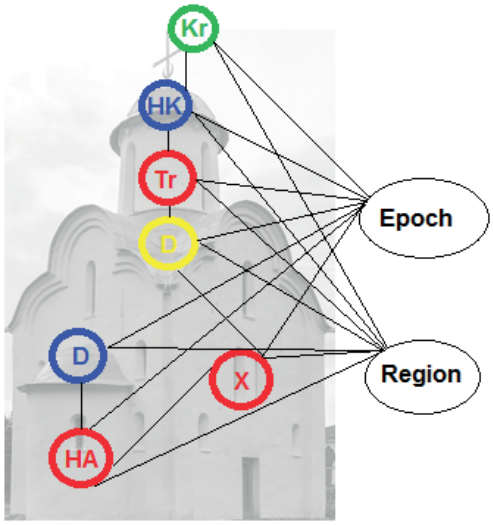

Figure 2. Church representation with a coloured graph.

We take into account the following encoding for the representation of some components:

- The letters in the vertices are the specific structural components with a specific geometry and localization.
- The edges, coded with a line, show the topological and probabilistic connection or the probabilistic influence of the components on each other (for example, if one component were detected, then we can claim, with a defined probability, that another component must be detected or reconstructed and vice versa).
- For visual comfort, we represent the different geometry types with different colours, i.e., each class of detected geometry type has its own colour.

2.4. Mathematical Background

Let us consider a mathematical method solving a decision problem correctly. This means, in the context of our research, that we have checked the information about some parts of our object, we can apply the arbitrary method of recognition and search an object in a certain place. Consider a method based on the use of Bayesian networks as one method to guide this search process.

We use the basic formula (Bayesian Theorem)

$$P(\theta \mid I) = \frac{P(\theta)P(\theta \mid I)}{P(I)} \tag{1}$$

where

- I is the information about those parts of an object, which were detected;
- $P(I)$ is the probability of I, defined as the frequency of objects, identified as I in all sets of churches;
- θ is the identifiers of those geometrical objects, which we want to detect;
- $P(I|\theta)$ is the posterior probability: the distribution element of object identifiers under the assumption of already detected objects;
- $P(\theta)$ is the prior probability: it is the formalization of our intuition about the possibility of the detection of an object. In our case, the value of this probability is defined statistically after the quantitative data analysis, after the supervision of such parts in orthodox churches.

All conditional probabilities are learnt from training datasets.

The expression $P(I|\theta)$ is called likelihood; it is a probability of a known data supervision by the fixation of certain identifiers. Thus, our task is to find the maximum a posteriori hypothesis θ, by which $P(\theta|I)$ is maximized.

If we set $P(I|\theta)$ of likelihood functions according to Equation (1), the decision problem is solved correctly. However, the establishment process of these functions is not a trivial procedure. These distributions can be rather difficult.

If we add some additional restrictions, the problem of $P(I|\theta)$ - function calculation can be simplified. By the conditional independence $a_1, a_2, \ldots a_n$ of the object identifiers, which define I, we have:

$$P(a_1, a_2, \ldots a_n | \theta = \theta k) = P(a_1 | \theta k)P(a_2 | \theta k)\ldots P(a_n | \theta k) \tag{2}$$

If I contains information in our case that $X = X_1$ (an event a_1), $HK - St = HK - St_1$ (an event a_2), and $\theta = \theta_k$ means that $D = D_k$, then $P(I|\theta = \theta_k)$ is the multiplication of the two probabilities of $P(a_1|\theta = \theta_k)$ and $P(a_2|\theta = \theta_k)$. Each of these probabilities will be defined from the set of those churches, at which X_1, $HK - St_1$ respectively among those churches, at which $D = D_k$.

In our example, we can find the subgraphs shown in Figure 3.

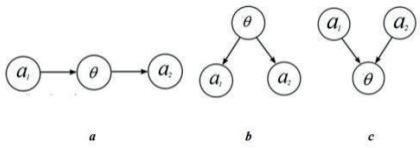

Figure 3. Subgraphs of the probability connections.

The pointers on the graph edges are suspended in most of the cases of this article. The graph of Figure 3a corresponds to the expression in Equation (2):

$$P(a_1, \theta, a_2) = P(a_1)\, P(\theta \mid a_1)\, P(a_2 \mid \theta)$$

From this follows

$$P(I \mid \theta) = P(a_1, a_2 \mid \theta) = \frac{P(a_1, \theta, a_2)}{P(\theta)} = \frac{P(a_1) P(\theta \mid a_1) P(a_2 \mid \theta)}{P(\theta)} = P(a_1 \mid \theta) P(a_2 \mid \theta) \tag{2a}$$

Because

$$\frac{P(a_1) P(\theta \mid a_1)}{P(\theta)} = P(a_1 \mid \theta)$$

according to the Bayes Theorem (cf. Equation (1)).

The graph of Figure 3b defines the following equality:

$$P(\theta, a1, a2) = P(\theta)\, P(a1 \mid \theta)\, P(a2 \mid \theta) \tag{3}$$

resulting in

$$P(I \mid \theta) = P(a_1, a_2 \mid \theta) = \frac{P(\theta, a_1, a_2)}{P(\theta)} = \frac{P(\theta) P(a_1 \mid \theta) P(a_2 \mid \theta)}{P(\theta)} = P(a_1 \mid \theta) P(a_2 \mid \theta) \tag{3a}$$

This simplifies the likelihood functions. When a_1 and a_2 influence θ at the same time (Figure 3c), it is possible to express this by

$$P(a1, a2, \theta) = P(a1)\, P(a2)\, P(\theta \mid a1, a2) \tag{4}$$

In this case, we receive a likelihood function which depends on the intended value, which, obviously, does not yield the correct decision. The likelihood function will be calculated directly.

A similar approach will allow us to optimize the procedure of this method choice for object extrapolation.

2.5. Processing Principles

Let us consider the graph which describes an input church as a special type of cellular automaton. As described above, cellular automaton is a discrete model for the description of dynamic systems consisting of spatial discrete cells, for which the state of time $t + 1$ depends on the states of cells in the neighbourhood and its own state of time t.

A cellular automata has the following characteristics:

- Cellular lattice/space R (Bayesian network with a certain number of churches)
- Final neighbourhood B (number of vertices in the Bayesian network)
- States amount k (probable geometries of church components in the network)

- Local transition function σ

The church graph is a lattice of cellular automaton, in which vertices are the automata cells. The cellular automaton can be defined as a set of final automatas with concrete state in discrete time t:

$$\sigma \in \Sigma = \{0, 1, 2 \ldots k-1, k\} \tag{5}$$

A detection of component geometries changes the automaton states of each cell in the neighbourhood according to the transition rule:

$$\sigma i, j(t+1) = \emptyset(\sigma k(t) \mid \sigma k(t) \in N) \tag{6}$$

N is the set of automatas that constitute a neighbourhood. At time t, we have three kinds of cells:

1. cells with an unambiguously defined state (e.g., detected geometry);
2. "pending" cells which incident (but do not belong) to defined cells;
3. "empty" cells which do not incident and do not belong to defined cells.

In our case, we set an initial state randomly. It is reasonable to set the most probable state as the initial state: it means that the search is statistically driven, starting with the most likely geometry for each component. The transition function will be defined; if the vertex B does not belong to N, there are edges from the vertex B incidental to the vertices from N ("pending cells"):

The state of the vertex is

$$B = \begin{cases} B_1, P_1 = P(B_1 \mid N) \\ B_2, P_2 = P(B_2 \mid N) \\ \ldots \\ B_k, P_k = P(B_k \mid N) \end{cases} \tag{7}$$

If the vertex B belongs to N, the state of a vertex remains the same with the probability of 1 (almost sure event). If the vertex B has no edge with any vertex from N, the state of a vertex remains the same with the probability of 1.

Applying the Maximum-Likelihood method, we choose the state in the pending vertices with respect to the maximum of the corresponding probabilities $B_k = \{B_i, max(P_i) = P_k\}$ and check for the correctness. It defines appropriate processes in all pending vertices, in which we detect the geometry of the church structural element by the method chosen according to a state. The following results are possible:

1. The geometry in the pending vertex has been detected. In this case, we attach a vertex to the N-set.

2. The geometry in the pending vertex has not been detected with the method chosen according to a state (we define this state as B_1 without loss of generality).

Let us transform the transition function: If the vertex B does not belong to N, there are edges from the vertex B incidental to vertices from N ("pending vertices") and in the previous step this vertex was not a pending vertex.

The state of the vertex is:

$$B = \begin{cases} B_1, P_1 = P(B_1 \mid N) \\ B_2, P_2 = P(B_2 \mid N) \\ \dots \\ B_k, P_k = P(B_k \mid N) \end{cases} \tag{7a}$$

If the vertex B does not belong to N, there are edges from the vertex B incidental to the vertices from N ("pending vertices") and in the previous step this vertex was a pending vertex.

The state of the vertex is:

$$B = \begin{cases} B_2, P_2 = P(B_2 \mid N, not \quad B_1) \\ \dots \\ B_k, P_k = P(B_k \mid N, not \quad B_2) \end{cases} \tag{7b}$$

If the vertex B belongs to N, the state of a vertex remains the same with the probability of 1. If the vertex B has no edge with any vertex from N, the state of a vertex remains the same with the probability of 1.

This iterative process yields a distinct solution since all cells will finally change their state to "unambiguously defined". In our case, it is convenient to visualize the state of a vertex with a colour. To each state of B_k, a specific colour is assigned. Thus, the presented probabilistic automaton presents the process of vertex colouring in the graph.

3. Tests

In this section, we will present the test results of our probabilistic automaton, which is based on the real data. For the test, we have chosen the Russian Orthodox Church in Wiesbaden (Germany) that completely conforms to the orthodox construction canons and Russian church typology. The Russian Orthodox Church in Wiesbaden was built in 1855. The church has not been destroyed and is well maintained. However, the golden domes and roof have incorrectly reflected laser beams and therefore there is a gap in the church point cloud (see Figure 4). It was a suitable case to verify our algorithm.

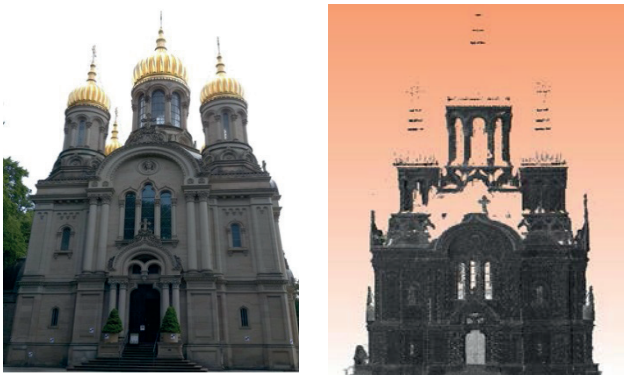

Figure 4. Russian church in Wiesbaden (left) and its point cloud with gaps (right).

To realize the algorithm, we applied a database of 50 orthodox churches that contains information about the semantics and geometry of church components, which have been manual entered. A joint graph, which includes church component frequencies (probability of its occurrence among 50 churches in the database), is calculated based on information in the database (see Figure 5). Further, the data in a joint graph serves to detect geometries of destroyed or lacking components.

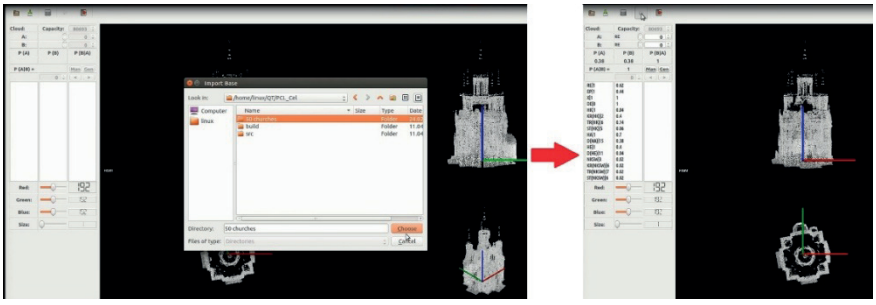

Figure 5. Generation of a joint graph with component probabilities.

As previously stated, only the reconstruction algorithm is realized in this article, which does, however, require some pre-processing steps, such as segmentation, semantic definition etc., that are not automatically realized at this moment. Therefore, these steps will be made manually. According to the classification library (see above), some church components can be visually detected in the point cloud of the Wiesbaden church (see Table 2, Figure 6):

Table 2. Visual detection of church component geometries corresponding to the classification library.

PC Sample	Pattern	ID	Vertex Type
		Tr 3	Tr
		$X1$	X
		HA 2	HA
		$D1$	D

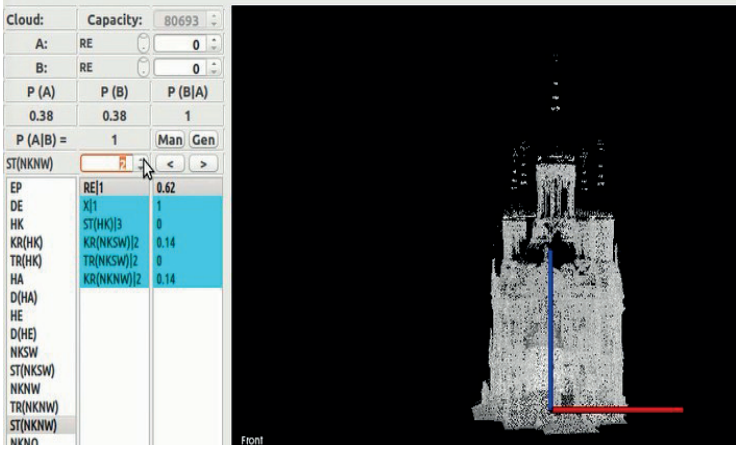

Figure 6. Manual generation of a test graph.

Certain components, e.g., domes and crucifixes, were not scanned correctly and make a gap in the church point cloud. Let us try to reconstruct the geometries of these components using our algorithm. The information about geometries and the semantic of "detected" church components, that we have visually defined, will be entered manually according to our graph construction rules. Based on such "detected" components, the automation completes the test graph of the input church with the most probable missed components, which can be presented through the schema of graph colouring (Figure 7).

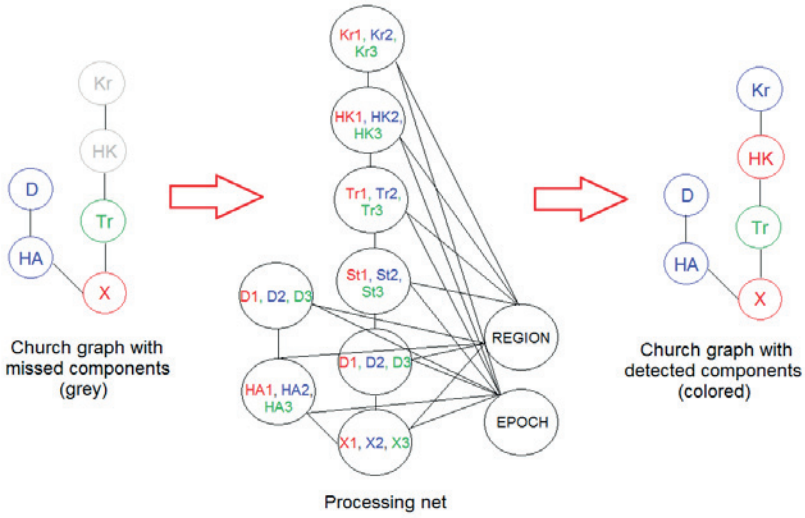

Figure 7. Schematic representation of the detection process.

To verify the algorithm, we used a one-step automaton, which generated the most probable geometries of missing components. In this article, we have not imitated the conflicts in the case of an unsuccessful geometry detection from a real point cloud, because our goal is to compare the results proposed from an automaton with the original church. Based on "detected" components, the algorithm proposed the most probable component geometries, which conform to the component geometries of the original church (Figures 8 and 9).

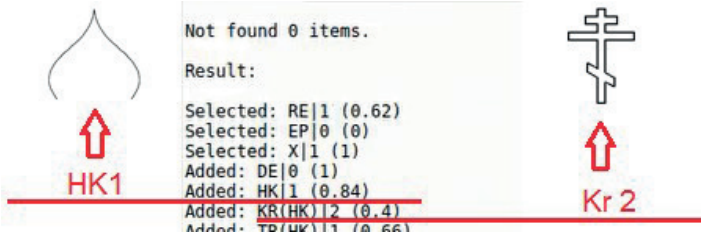

Figure 8. Correct detected geometries of missing parts.

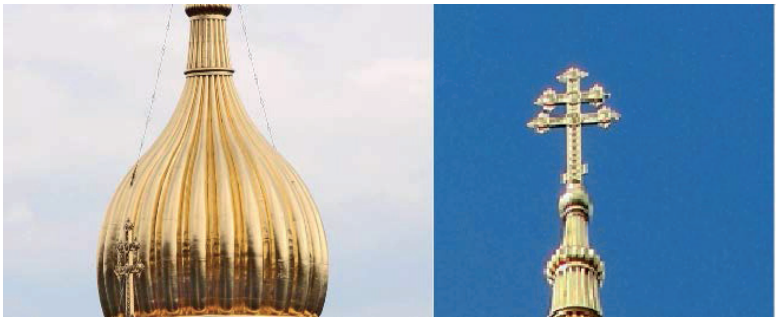

Figure 9. Original church parts.

4. Conclusions

We developed a mathematical theory and showed the feasibility of an approach to simulated data of stone Russian Orthodox churches. The presented method allows an automatic reconstruction of the whole complex object with missing components on the basis of the iterative detected geometries of its components. The method's principles are universal and applicable for other types of objects (this would require additional libraries of structural components and component relations in the graph). The results of this algorithm depend on the quality of pre-processing steps, especially correct geometry detection and semantic definition of the church parts.

Further work will be concentrated in two directions: On the one hand, empirical work on the correct segmentation and semantic definition of the church parts. On the other hand, the cellular automaton will be realized for larger and more complex building models with consideration of conflicts such as the presence of new objects, which were not described in our classification library, or the absence of some components that were not planned for in some church constructions.

Acknowledgements: We thank the Free State of Bavaria, who made this research possible by a grant for the visit of Prof. Korovin at the FHWS.

References

1. Ahn, S. *Least Squares Orthogonal Distance Fitting of Curves and Surfaces in Space*; Springer: Berlin, Germany, 2004.
2. Al-Durgham, K.; Habib, A.; Kwak, E. Ransac approach for automated registration of terrestrial laser scans using linear features. *ISPRS Ann. Photogramm. Remote Sens. Spat. Inf. Sci.* **2013**, *II*, 13–18.

3. Anand, A.; Koppula, H.; Joachims, T.; Saxena, A. Contextually guided semantic labeling and search for three-dimensional point clouds. *Int. J. Robot. Res.* **2013**, *32*, 19–34.
4. Arefi, H.; Hahn, M.; Reinartz, P. Ridge based decomposition of complex buildings for 3d model generation from high resolution digital surface models. *Int. Arch. Photogramm. Remote Sens. Spat. Inf. Sci.* **2010**, *34*, 15–22.
5. Becker, R. Differentialgeometrische Extraktion von 3D-Objektprimitiven aus terrestrischen Laser- scannerdaten. Ph.D. Thesis, Veröffentlichungen des Geodätischen Instituts der Rheinisch-Westfälischen Technischen Hochschule, Aachen, Germany, 2005. Available online: https://www.deutsche-digitale-bibliothek.de/binary/WI6IH566CY75KXJY3QX JBTG- MXWKJI5TS/full/1.pdf.
6. Canciani, M.; Falcolini, C.; Saccone, M.; Spadafora, G. From point clouds to architectural models: algorithms for shape reconstruction. *Int. Arch. Photogramm. Remote Sens. Spat. Inf. Sci.* **2013**, *XL*, 27–34.
7. Dore, C.; Murphy, M. Semi-automatic modeling of building facades with shape grammars using historic building information modeling. *Int. Arch. Photogramm. Remote Sens. Spat. Inf. Sci.* **2013**, *XL*, 57–64.
8. Dore, C.; Murphy, M.; McCarthy, S.; Brechin, F.; Casidy, C.; Dirix, E. Structural simulations and conservation analysis of historic building information model (HBIM). *Int. Arch. Photogramm. Remote Sens. Spat. Inf. Sci.* **2015**, *XL*, 351–357.
9. Fleischmann, S.; Cohen-Or, D.; Silva, C. Robust moving least-squares fitting with sharp features. *Proc. ACM SIGGRAPH* **2005**, *24*, 544–552.
10. Förstner, W. Graphical models in geodesy and photogrammetry. *PFG Photogramm. Fernerkund. Geoinform.* **2013**, *4*, 255–267.
11. Huang, H.; Brenner, C.; Sester, M. 3d building roof reconstruction from point clouds via generative models. In Proceedings of the 19th ACM SIGSPATIAL International Conference on Advances in Geographic Information Systems, Chicago, IL, USA, 1–4 November 2011; pp. 16–24.
12. Kada, M.; Wichmann, A. Feature-driven 3d building modeling using planar. *Int. Arch. Photogramm. Remote Sens. Spat. Inf. Sci.* **2013**, *II-3/W3*, 37–42.
13. Kivilcim, C.; Duran, Z. A semi-automated point cloud processing methodology for 3d cultural heritage documentation. *Int. Arch. Photogramm. Remote Sens. Spat. Inf. Sci. 2016*, *XLI*, 293–296.
14. Koller, D.; Friedman, N. *Probabilistic Graphical Models: Principles and Techniques*; MIT Press: Cambridge, MA, USA, 2009.
15. Liu, Y.; Wang, W. Advances in Geometric Modeling and Processing. In *Springer Berlin Heidelberg, chapter A Revisit to Least Squares Orthogonal Distance Fitting of Parametric Curves and Surfaces*; Springer: Berlin/Heidelberg, Germany, 2008; pp. 384–397.
16. Maltezos, E.; Ioannidis, C. Automatic extraction of building roof planes from airborne LiDAR data applying an extended 3d randomized Hough transform. *Int. Arch. Photogramm. Remote Sens. Spat. Inf. Sci.* **2016**, *III*, 209–216.
17. Neapolitan, R.E. *Learning Bayesian Networks*; Pearson Prentice Hall: Upper Saddle River, NJ, USA, 2004.

18. Nguatem, W.; Drauschke, M.; Mayer, H. Roof reconstruction from point clouds using importance sampling. *Int. Arch. Photogramm. Remote Sens. Spat. Inf. Sci.* **2013**, *II*, 73–78.
19. Nizar, A.A.; Filin, S.; Doytsher, Y. Reconstruction of buildings from airborne laserscanning. In Proceedings of the ASPRS Annual Conference, Reno, NV, USA, 1–5 May 2006; pp. 106–115.
20. Overby, J.; Bodum, L.; Kjems, E.; Ilsoe, P. M. Automatic 3d building reconstruction from airborne laserscanning and cadastral data using Hough transform. *Int. Arch. Photogramm. Remote Sens. Spat. Inf. Sci.* **2004**, *XXXV*, 296–301.
21. Quattrini, R.; Malinverni, E.S.; Clini, P.; Nespeca, R.; Orlietti, E. From TLS to HBIM: high quality semantically-aware 3d modelling of complex architecture. *Int. Arch. Photogramm. Remote Sens. Spat. Inf. Sci.* **2015**, *XL*, 367–374.
22. Rabbani, T.; Heuvel, F. Efficient Hough transform for automatic detection of cylinders in point clouds. *Int. Arch. Photogramm. Remote Sens. Spat. Inf. Sci.* **2005**, *XXXVI*, 60–65.
23. Ruiz-Sarmiento, J.; Galindo, C.; Gonzalez-Jimenez, J. Scene object recognition for mobile robots through semantic knowledge and probabilistic graphical models. *Exp. Syst. Appl.* **2015**, *42*, 8805–8816.
24. Rusu, R.; Blodow, N.; Marton, Z.C.; Beetz, M. Close-range scene segmentation and reconstruction of 3d point cloud maps for mobile manipulation in domestic environments. In Proccedings of the International Conference on Intelligent Robots and Systems, St. Louis, St. Louis, MO, USA, 10–15 October 2009; pp. 1–6.
25. Schnabel, R.; Wahl, R.; Klein, R. Efficient RANSAC for point-cloud shape detection. *Comput. Graph. Forum* **2007**, *26*, 214–226.
26. Neumann, J. *Theory of Self-Reproducing Automata*; University of Illinois Press: Champaign, IL, USA, 1966.
27. Verma, V.; Kumar, R.; Hsu, S. 3d building detection and modeling from aerial LiDAR data. In Proceedings of the 2006 IEEE Computer Society Conference on Computer Vision and Pattern Recognition, New York, NY, USA, 17–23 June 2006; Volume 2, pp. 2213–2220.
28. Vosselman, G.; Gorte, B.; Sithole, G.; Rabbani, T. Recognising structure in laser scanner point clouds. *Int. Arch. Photogramm. Remote Sens. Spat. Inf. Sci.* **2004**, *XXXVI*, 33–38.
29. Wang, W.; Pottmann, H.; Liu, Y. *Fitting B-Spline Curves to Point Clouds by squared Distance Minimization*; Technical Report, HKU CS Tech Report TR-2004-11; 2004. Available online: http://www.cs.hku.hk/research/techreps/document/TR-2004-11.pdf.
30. Wolfram, S. Statistical mechanics of cellular automata. *Rev. Modern Phys.* **1983**, *55*, 601–644.
31. Xiong, B.; Jancosek, M.; Elberink, S.O.; Vosselman, G. Flexible building primitives for 3d building modeling. *ISPRS J. Photogramm Remote Sens.* **2015**, *101*, 275–290.
32. Xiong, X.; Huber, D. Using context to create semantic 3d models of indoor environments. In Proceedings of the British Machine Vision Conference (BMVC), Wales, UK, 30 August–2 September 2010; pp. 1–11.

Chizhova, M.; Korovin, D.; Gurianov, A.; *et al.* A general Approach for the Reconstruction of Complex Buildings from 3D Pointclouds Using Bayesian Networks and Cellular Automata. In *Latest Developments in Reality-Based 3D Surveying and Modelling*; Remondino, F., Georgopoulos, A., González-Aguilera, D., Agrafiotis, P., Eds.; MDPI: Basel, Switzerland, 2018; pp. 74–92.

© 2018 by the authors. Licensee MDPI, Basel, Switzerland. This article is an open access article distributed under the terms and conditions of the Creative Commons Attribution (CC BY) license (http://creativecommons.org/licenses/by/4.0/).